

INFLUENCE OF Ti DOPING ON THE OPTICAL AND STRUCTURAL PROPERTIES OF ZnTiO THIN FILMS DEPOSITED BY ELECTRODEPOSITION TECHNIQUE

Abstract

Thin films of titanium doped zinc oxide (Ti-ZnO) have been successfully deposited on fluorine doped tin oxide (FTO) conductive glass substrate using electrodeposition method to study the effects of Ti doping on ZnO films in this work. Zinc acetate and titanium powder digested with hydrogen fluoride were the starting materials used for Zn, Ti and O ions sources. Volume concentration of Ti ions source was varied with very slight change in the source of Zn and O ions. The electrodeposition setup involved three electrodes system in which the FTO was used as working electrode while platinum rod and Ag/AgCl were used as the counter and reference electrodes respectively. The deposited thin films of Ti-ZnO were characterized for their optical and structural properties using UV-Vis spectrometry and X-ray diffraction technique respectively. The results of the characterizations showed that the optical properties of the films such as transmittance, refractive index, extinction coefficient and bandgap energy were influenced by Ti doping. The transmittance (%) was found to decrease for the film (10 ml Ti/ZnO) deposited at highest Ti concentration in the VIS region but increased to the highest value in the NIR region. The bandgap energy of the deposited thin films was found to decrease with an increase in the volume concentration of Ti doping and the obtained values were (2.73 – 3.20 eV) for undoped ZnO sample, (2.73 – 3.18 eV) for 4 ml Ti/ZnO, 3.0 eV for 6 ml Ti/ZnO, 2.81 eV for 8 ml Ti/ZnO and 2.76 eV for the film 10 ml Ti/ZnO. The structural analysis via X-ray diffraction indicated that the fabricated films have crystalline structures which are also influenced by Ti doping. The crystallite size of the films was found to increase while micro-strain decreased as doping concentration increased which signified improvement in crystal structure for device applications. These obtained results positioned the deposited thin films of Ti-doped ZnO for wide range of electronic and opto-electronic device applications.

KEYWORDS: Zinc Oxide ZnO, Titanium, Transparent Conducting Oxides (TCOs), Wide Bandgap, Opto-electronics.

1.0 Introduction

Thin films of most metal oxide of group II elements have been known to demonstrate vast potential applications in diverse fields of science and technology today. Some of these fields of applications of these sets of materials are electronics and opto-electronic devices fabrications, medicine/medical device treatment and in military/defense etc. [1-3]. The group II metal oxides that are of interest for these purposes include but not limited to cadmium oxide (CdO), magnesium oxide (MgO), zinc oxide (ZnO), etc. These metal oxide films have been noted to possess a peculiar characteristic necessary for vast scientific and technological applications. In particular, most thin films of these metal oxides have unique combination of electrical conductivity and optical transparency and are thus well known as transparent conductive oxides (TCOs) and demonstrate quite vital roles for many opto-electronic device applications such as light emitting diodes (LEDs) and solar cells, [4]. In addition to high transparency, most group II metal oxides are known to exhibit direct wide bandgap energy values which positioned them for the varieties of potential applications credited to them. (ref). [5, 6]. However, adding to some of these common characteristics attributable to most of the group II metal TCOs, each of these materials has been identified to still have some peculiar features that make them favorable for a given application. ZnO is one of the prominent members of the group II metal oxide family that have been identified to exhibit some excellent characteristics favorable for many technological applications compared to others. Adding to the common high transparency properties and large bandgap energy values of group II metal TCOs, ZnO material has also been known to possess very large value of exciton binding energy of about 60 MeV which is quite larger than the values for other II metal oxides at room temperature and high electron mobility, [7]. The material is nontoxic in nature, less expensive and equally has

excellent chemical and thermal stability which make it suitable for many applications added to it. The bandgap energy of ZnO has been noted to be at least 3.2 eV at room temperature, [8,9]. The vast areas of applications of ZnO so far identified include; electronics, photovoltaic cells, optoelectronic components, Piezotronic and piezophototronic, gas sensors, photodetectors, optical coating devices, microelectronics, light emitting diodes, fuel cells, etc., [10]. However, with these numerous areas of device applications credited to ZnO material, the large bandgap energy value it possesses has constituted some drawbacks to its use in some other applications and thus need modification of its structure/properties. Doping of ZnO has been found to play an important role in tailoring the properties of ZnO thin films for suitable applications in many other areas. Research has shown that doped ZnO provides an excellent material system to precisely control the optical, electronic and magnetic properties of the materials for many different device applications. For instance, doping the material with some foreign element (impurity) aim at increasing the defects state in the material lattice, a higher electron-hole (e^-/h^+) pair can be generated and a reduction in the band-gap energy can be achieved, [11]. It has also been argued that doping 3d transition metal ions into ZnO structures provides an effective way to alter their electrical and magnetic properties and among the 3d transition metals, titanium (Ti) has been tipped to own several advantages over others for doping ZnO, [12]. Ti is a quadrivalent cation element and has ionic radius of 0.68 Å (68 pm) which is very close to that of Zn 0.74 Å (74 pm) and could be incorporated as an interstitial atom to act as a scattering site in ZnO. However, it has been reported that only a small amount of doped Ti^{4+} will induce more electrons thereby stopping it to act as scattering centers, [13]. The quadrivalent cation Ti^{4+} provides two free electrons to contribute to conduction as it substitutes Zn ion in ZnO films. In nutshell, Ti^{4+} replaces Zn^{2+} in the valence band and therefore provides more than one electron in the conduction band. This allows increasing the conductivity by using a lower concentration of the dopant Ti, hence it is a suitable donor in ZnO as compared to other transition metals. This feature allows the incorporation of Ti ions into ZnO lattice and improves its properties [14, 15]. Several methods have been utilized to fabricate thin films of ZnO doped with Ti via different deposition parameters/conditions and quite different results have been achieved and reported, [16-24]. In this report, we employed cost effective electrodeposition method to deposit thin films of Ti-ZnO by varying their volume concentrations to study their effects on the optical and structural properties.

2.0 Materials and Method

The starting materials used for the deposition of the Ti-doped ZnO thin films include the following; zinc acetate (source of Zn and O ions), titanium powder (Ti ion source) and hydrogen fluoride (digestor). Other materials used were fluorine-doped tin oxide (FTO) conductive glass substrate: - used as working electrode, silver/silver chloride (Ag/AgCl):- served as reference electrode, platinum rod: - used as the counter electrode, 100 ml glass beaker: - used as reaction bath, distilled water: - used as the reaction medium, Potentiostat (model Zhaoxin: RXN-3010D):- DC supply unit and magnetic stirrer

The method employed in the deposition of the thin films is electrodeposition method with three electrodes configuration. To deposit the zinc oxide thin film on FTO substrate via this method, aqueous electrolytic bath solution of 40 ml 1.0 M of zinc acetate was used. The three electrodes were immersed into the bath containing the electrolytic solution and 3.5 volts was maintained from the DC supply unit setup for 60 seconds. In synthesizing the Ti-doped ZnO thin films, different volume concentrations of Ti ion precursors of 10 ml, 8 ml, 6ml and 4 ml were introduced into the electrolytic bath containing zinc acetate solution and the 3.5 volts was again maintained from the DC supply unit setup for 60 seconds each. The details of the experimental procedure for the fabrication of the thin films of Ti-ZnO is summarized in Table 1.

Table 1: Bath parameter for optimization of Ti-ZnO thin films

1.0 M $Zn(C_2H_3CO_2)_2 \cdot 2H_2O$	2.5g Rutile + 50ml HF+1hr stir with magnetic stirrer	Applied potential	Time
Vol. (ml)	Vol. (ml)	Volts	(sec.)

30.00	10.00	3.5	60.0
32.00	8.00	3.5	60.0
34.00	6.00	3.5	60.0
36.00	4.00	3.5	60.0
40.00	0.00	3.5	60.0

The deposited thin films were characterized for their optical and structural properties using UV-Vis spectroscopy and X-ray diffraction method respectively.

3.0 Results and Discussion

3.1 Optical Properties of deposited ZnO and Ti-doped ZnO thin films

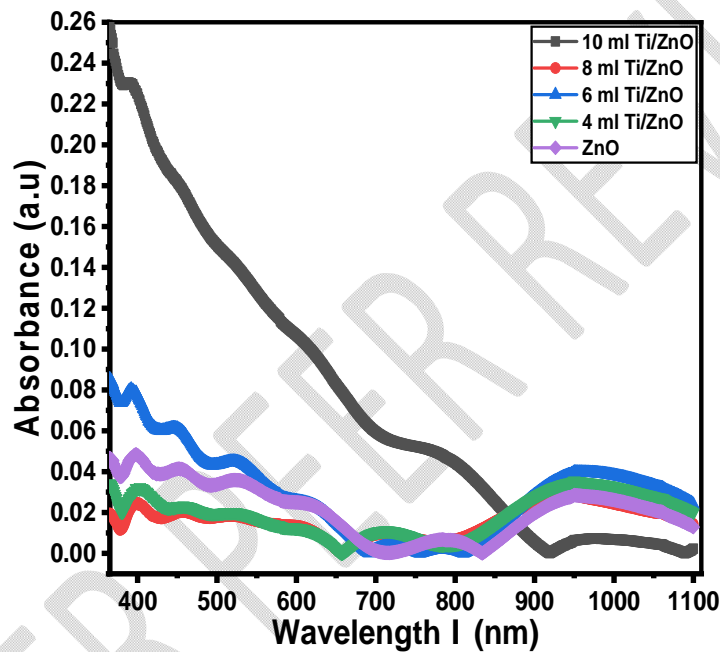


Figure 1: Graph of Absorbance against wavelength for the Ti/ZnO thin films

Figure 1 is the graph of absorbance as a function of wavelength for the deposited thin films of Ti doped ZnO. The absorbance was obtained by measuring its values directly from the UV-VIS spectrometer machine. From the figure, it is observed that the deposited thin films have very low absorbance within the visible and near infrared (VIS and NIR) regions of electromagnetic spectrum. However, the film deposited at higher concentration of Ti doping (10 ml Ti doped ZnO) has an increased absorbance value in the range of 0.05 to 0.26 in the VIS region and thereafter decreased to lowest value in the NIR region.

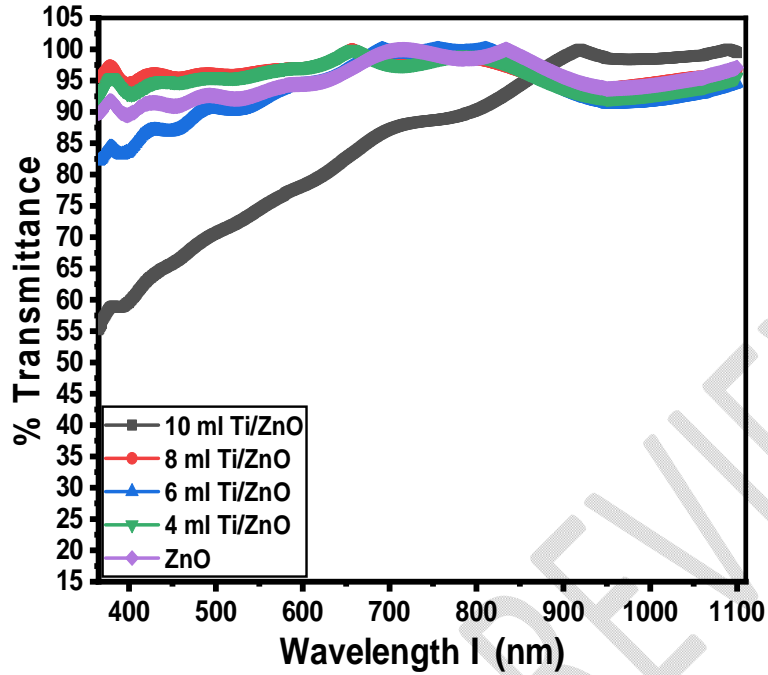


Figure 2: Graph of % Transmittance against wavelength for the Ti/ZnO thin films

The plot of percentage transmittance of the films as a function of wavelength is displayed in figure 2. The transmittance was obtained using the relation as given by [25, 26].

$$T = 10^{-A} \quad \text{-----} \quad 1$$

Where A is the measured absorbance of the films.

The figure showed that the films have high transmittance in the range of 80% to 100% except for the sample 10 ml Ti/ZnO which had a decreased value down to the range 55% - 85% in the VIS range. The high transmittance value exhibited by the deposited thin films in the regions of electromagnetic spectrum position them to be used as transparent conductive films for window coating applications in the low temperature environments in order to boost their temperatures and for other various optoelectronic gadgets. The films that have similar transmittance very close to this work have been reported by [27].

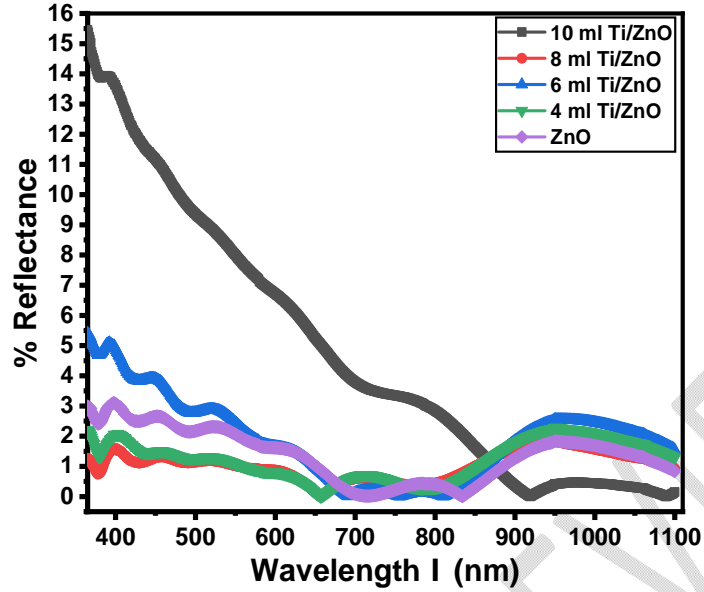


Figure 3: Graph of % Reflectance against wavelength for the Ti/ZnO thin films

The plot of percentage reflection of the films against wavelength is shown in figure 3 to determine the reflection properties of the deposited thin films of Ti/ZnO. The reflectance was estimated from the formula given by [28, 29].

$$R = 1 - \sqrt{\frac{e^A}{10^4}}$$

2

The percentage reflectance of the films is quite very low in the range of 1 -5% in the VIS and NIR regions, except for the film 10 ml Ti/ZnO which has increased value in the range 4 – 15.5% in the VIS region of electromagnetic spectrum. The low reflectance value of the films positioned them for anti-reflection coating application.

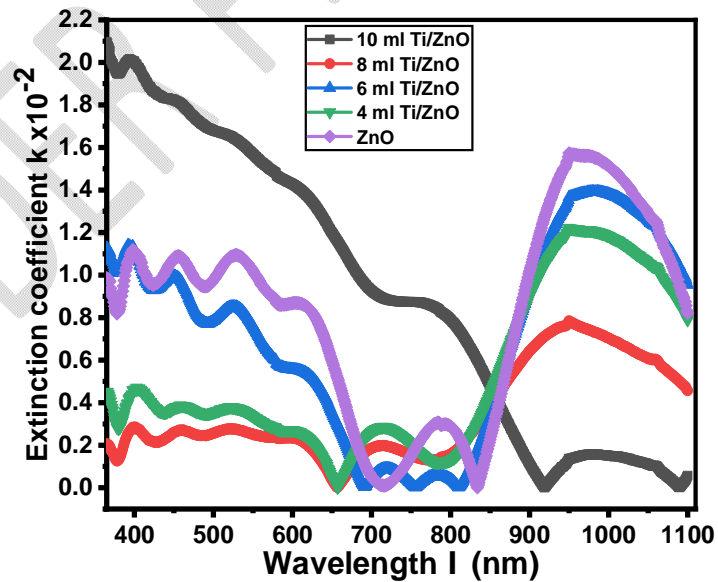


Figure 4: Graph of Extinction coefficient against wavelength for the Ti/ZnO thin films

The extinction coefficient of the deposited thin films Ti/ZnO is generally low as shown in figure 4. The extinction coefficient was evaluated using the relation as given by [30, 31].

$$k = \frac{\alpha\lambda}{4\pi} \quad 3$$

Where α is the absorption coefficient which was computed using the formula, [32].

$$\alpha = \frac{2.303A}{t} \quad 4$$

t is the film thickness which was obtained by gravimetric method and λ is the wavelength of UV-VIS light used.

From figure 4, it is observed that the extinction coefficient decreased within the VIS region and thereafter increased in the NIR to the peak value at wavelength 1000 nm. The extinction coefficient value is equally lowered as the concentration of the Ti doping increased in the NIR region of electromagnetic spectrum.

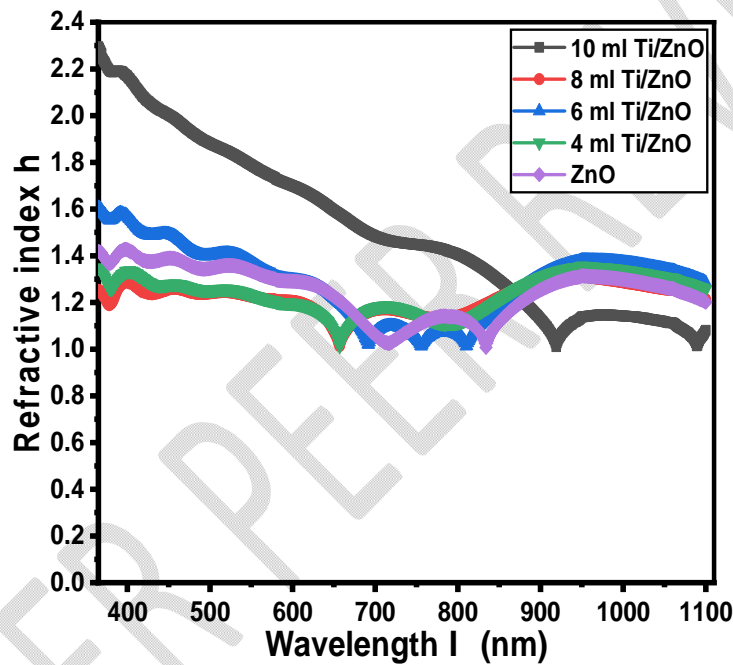


Figure 5: Graph of Refractive index against wavelength for the Ti/ZnO thin films

Figure 5 is the graph of refractive index of the deposited thin films of Ti/ZnO against wavelength to determine their effect on the speed of light. The refractive index was determined using the formula as provided by [33]

$$n = \frac{1+R^{0.5}}{1-R^{0.5}} \quad 5$$

Where R is the calculated value of the reflectance of the films.

The figure showed that the refractive index of the films is in the range of 1.0 – 1.6 except for the film 10 ml Ti/ZnO which has higher value in the range 1.5 – 2.3 in the VIS region and thereafter decreased to the value in the range 1.0 -1.2 in the NIR region of electromagnetic spectrum. These variations in the refractive index values of the films in different solar spectrum and at different molar concentrations of Ti doping showed that the Ti ions have effect on the ZnO film and the deposited films can be utilized for optical fiber and waveguide coating applications.

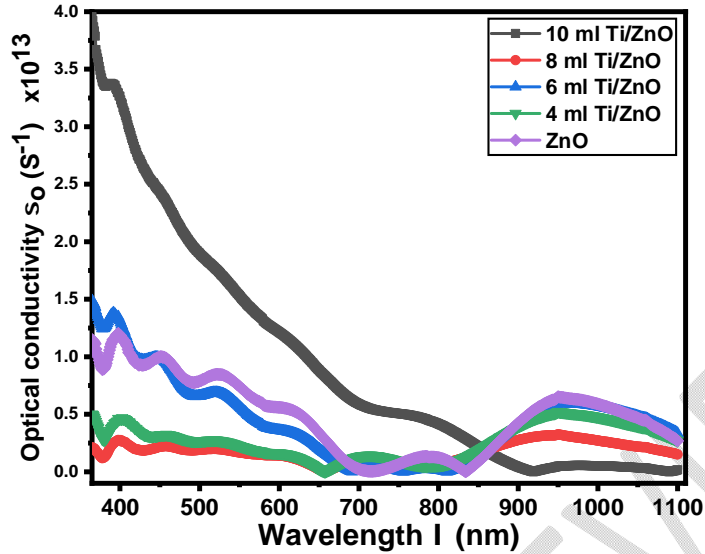


Figure 6: Graph of Optical conductivity against wavelength for the Ti/ZnO thin films

The plot of optical conductivity as a function of wavelength for the deposited thin films is displayed in figure 6. The optical conductivity was calculated from the relation given by [34, 35].

$$\sigma = \frac{\alpha n C}{4\pi}$$

6

Where n is the refractive index and C is the speed of light in vacuum. From the plot, the optical conductivity of the deposited thin films of Ti doped ZnO initially decreased with the concentration of Ti doping in the VIS region but increased to higher values in the range $0.75 - 4.0 \times 10^{13} \text{ S}^{-1}$ in the region. However, in the NIR region the optical conductivity was found to decreased purely as the doping concentration of Ti increased with the film 10 ml Ti/ZnO having the lowest value of the order $0.1 - 0.25 \times 10^{13} \text{ S}^{-1}$ while the un-doped ZnO has the highest value of about $0.75 \times 10^{13} \text{ S}^{-1}$ in the region.

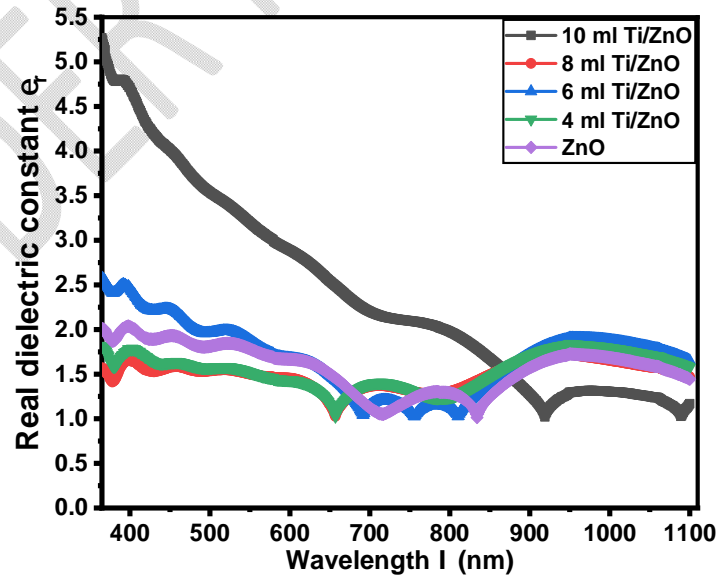


Figure 7: Graph of Real dielectric constant against wavelength for the Ti/ZnO thin films

Figure 7 represent the graph of real dielectric constant of the deposited thin films as a function of wavelength. The real dielectric constant of the films was estimated via the relationship as given by [36].

$$\epsilon_r = n^2 - k^2$$

7

Where n and k are the refractive index and extinction of the deposited thin films of Ti/ZnO. The figure showed that the real dielectric constant of the films decreased with an increase in wavelength in the VIS region with films 10 ml Ti/ZnO having the highest in the range 2.25 – 5.25 in the region while others have values in the range of 1.0 to 2.5. In the NIR region, the real dielectric constant of the films appeared to increased slightly to maximum of 2.0 at 950 nm and thereafter tend to decrease as wavelength increased in the region. The film 10 ml Ti/ZnO has the lowest value in the order of 1.0 – 1.5 and this indicated that at higher concentration of Ti doping, the real dielectric constant of the deposited films is lower in the NIR while in the VIS region they are higher.

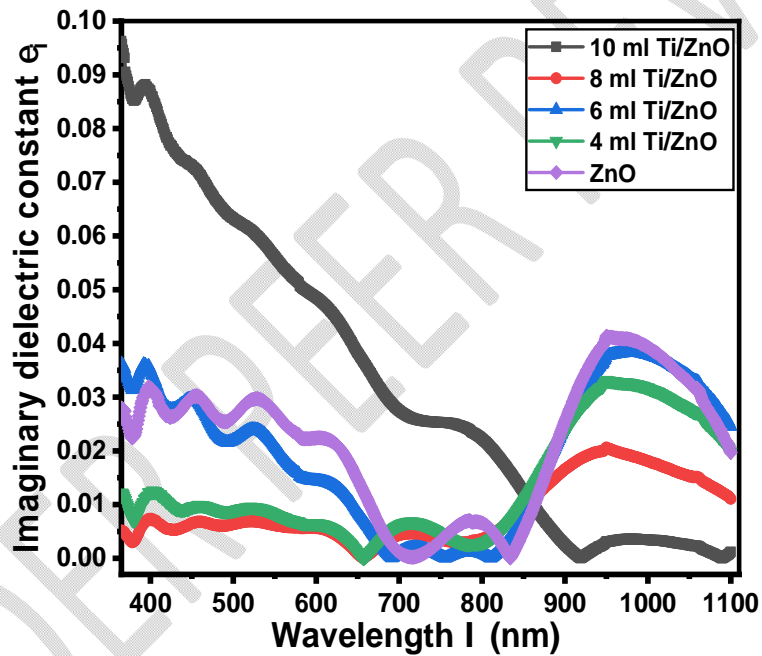


Figure 8: Graph of Imaginary dielectric constant against wavelength for the Ti/ZnO thin films

The graph of imaginary dielectric constant against wavelength is displayed in figure 8 for the deposited thin films of Ti doped ZnO. This property was calculated based on the relation given by[37].

$$\epsilon_i = 2nk$$

8

From the figure can be observed that the films have low values of imaginary dielectric constant which decreases with wavelength in the VIS region. The highest values of this property which range from 0.02 to 0.96 is exhibited by film 10 ml Ti/ZnO while others have values in the range 0.005 – 0.037 in the region. In the NIR region the imaginary dielectric constant of the films followed the same patterns as the real dielectric constant but tend to decrease with an increase in the concentration of Ti doping except for the film 6 ml Ti/ZnO which deviated from the trend.

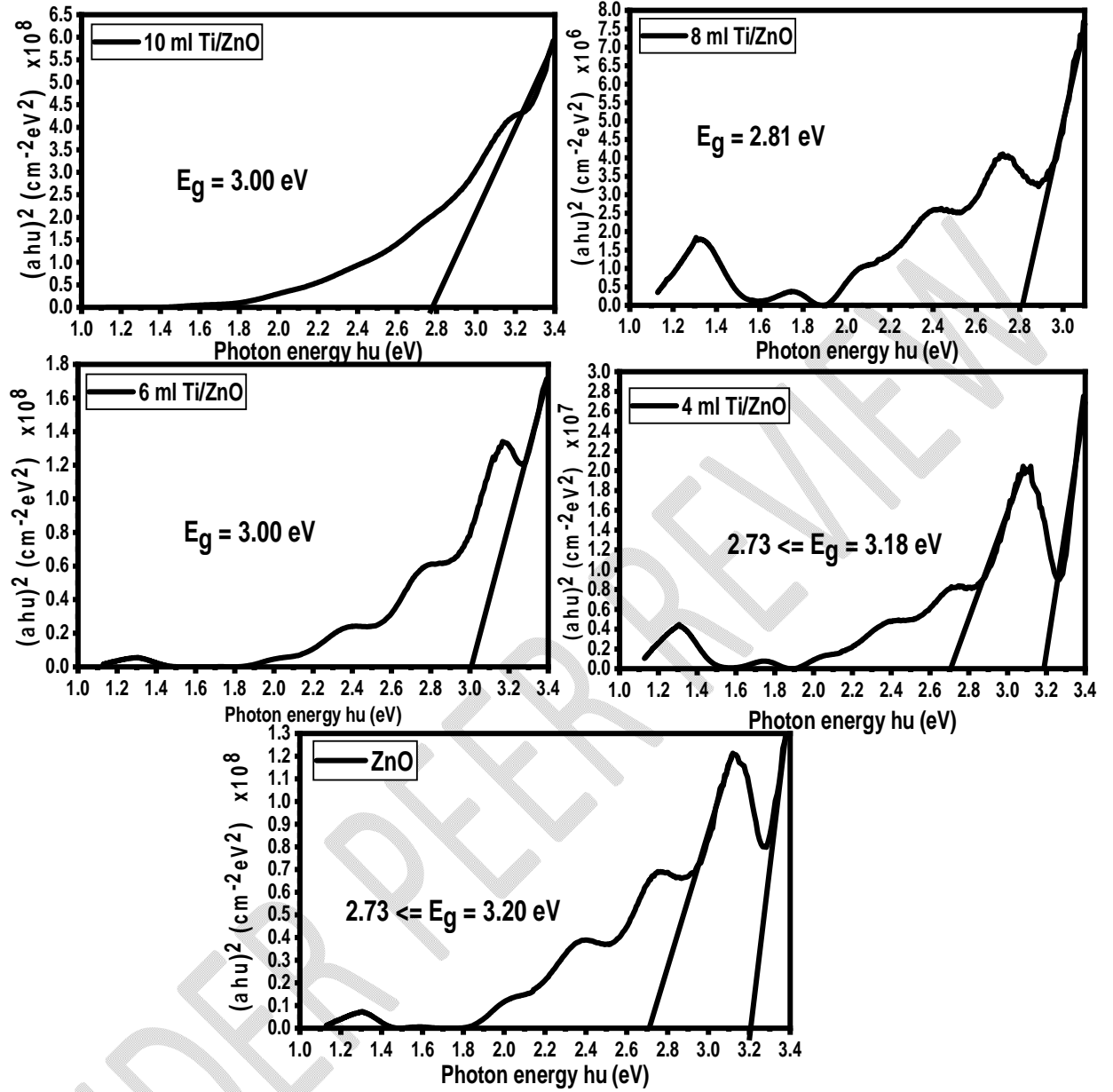


Figure 9: Plots of $(\alpha h\nu)^2$ as a function Photon energy for the Ti/ZnO thin films

Figure 9 is the plots of $(\alpha h\nu)^2$ as a function of photon energy to determine the bandgap energy of the deposited thin films of Ti/ZnO. The bandgap energy was calculated using the Tuac relation as given by [38, 39].

$$(\alpha h\nu)^n = \beta(h\nu - E_g)$$

9

Where E_g is the bandgap energy of the films, $h\nu$ is the photon energy, β is a constant while n is the transition factor which determine the nature of transition. For direct allowed transition, n takes the value 2 while for indirect transition it takes the value of $\frac{1}{2}$. From the plots in the figure, the bandgap energy values of the deposited thin film samples were estimated by extrapolating the straight-line portions of the curves on the photon energy axes at which

$(\alpha h\nu)^2$ equals to zero. The plots showed that the bandgap energies for un-doped ZnO sample is in the range 2.73 – 3.20 eV, 2.73 – 3.18 eV for 4 ml Ti/ZnO, the sample 6 ml Ti/ZnO has bandgap of 3.0 eV, 8 ml Ti/ZnO has bandgap of 2.81 eV while 10 ml Ti/ZnO has bandgap energy of 2.76 eV. These results showed that the bandgap energy of the deposited thin films of Ti/ZnO decreased with an increase in the concentration of Ti doping. These bandgap energies are wide bandgap values and thus position the deposited thin films for wide range of electronic and optoelectronic applications.

3.2 Structural properties of deposited Ti-doped ZnO thin films

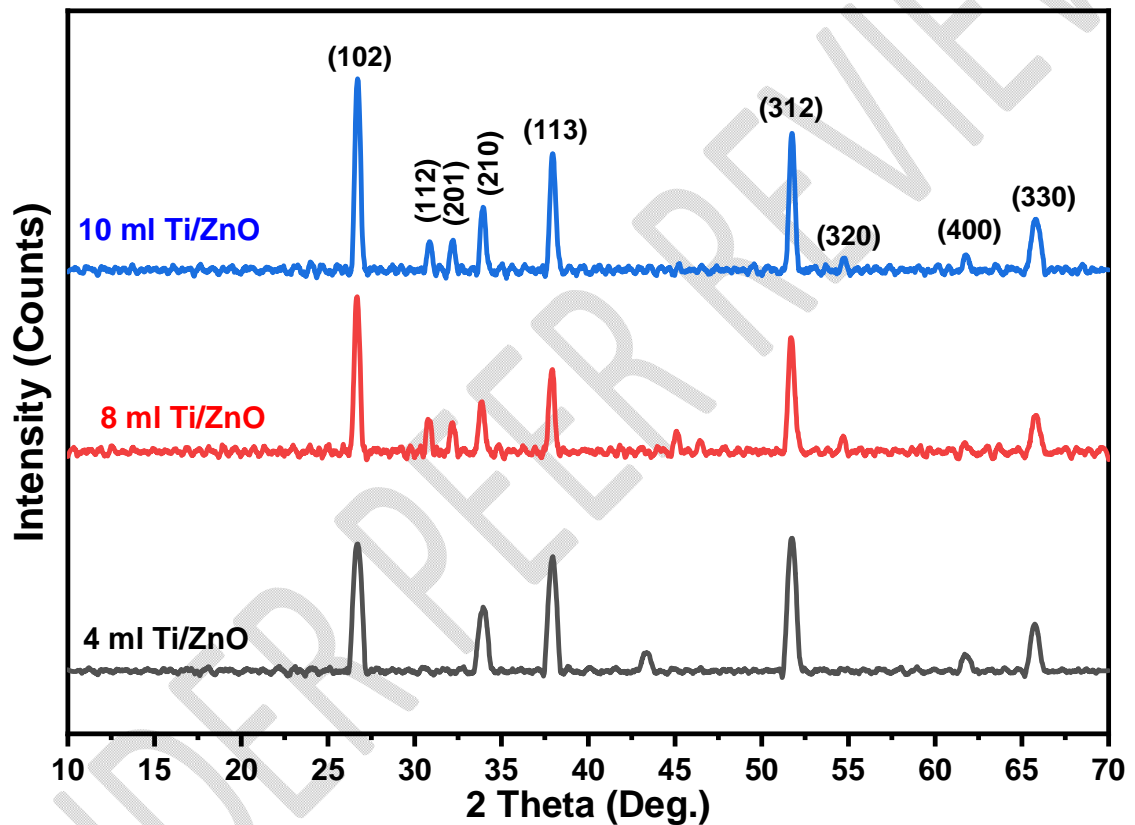


Figure 10: XRD pattern of the Ti/ZnO thin films

The XRD analysis patterns of the deposited thin films of Ti doped ZnO deposited with 4ml, 8ml and 10ml concentration of Ti source are displayed in figure 10. The results showed that the deposited thin films have crystalline structures with most preferential peaks having crystal planes (102), (113) and (312) occurring at two theta positions 26.78° , 37.99° and 51.75° respectively. There exist other minor sharp peaks in the XRD patterns of the films which are attributable to increase in the concentration of Ti doping in the films. These sharp peaks in the patterns of the films matched well with the (standard JCPDS NO: 00-154-4334, Space Group P4322 and crystal system: -Tetragonal structure). The Williamson-Hall (W-H) plots of the preferential peak positions for the films (figure 10) were used to estimate the crystallite sizes and the micro-stains of the deposited thin films of Ti/ZnO. The Williamson-Hall relation is as given by [40]

$$\beta_T \cos\theta = \frac{k\lambda}{D} + 4\varepsilon \sin\theta$$

10

Where β_T is the full width at half maximum (FWHM) obtained by running Gaussian linear fits at the two theta peak positions, θ is the Bragg's angle (half two-theta position), k is the shape factor with constant value 0.9, λ is the wavelength of the X-ray Cu- α radiation used to probe the thin film materials, D represents the crystallite size of the films and ε stands for the micro-strain of the films. From the W-H relation, the scatter plot of $\beta_T \cos\theta$ on the vertical axis and $4\sin\theta$ on the horizontal axis gives a straight-line graph subject to linear fits of the plots, with $\frac{k\lambda}{D}$ representing the intercept on the vertical axis while the micro-strain ε become the slope of the plot. From the W-H plots of the deposited thin films, the crystallite sizes were evaluated as 14.04 nm, 28.80 nm and 32.57 nm for 4ml, 8ml and 10ml Ti/ZnO films respectively. The micro-strains are (-1.047×10^{-3}) , 6.29×10^{-2} and 1.068×10^{-3} for 4ml, 8ml and 10ml Ti-doping respectively. The negative value for the films 4 ml Ti/ZnO suggests compressive strain in the film. The dislocation density (δ) of the films was also estimated based on the Wilson equation provided by[41].

$$\delta = \frac{1}{D^2} (\text{lines}/\text{nm}^2)$$

11

Where D is the estimated crystallite size from the H-W plots. The calculated values of the dislocation densities of the films are 5.07×10^{-3} lines/nm², 1.21×10^{-3} lines/nm² and 9.43×10^{-4} lines/nm² for 4ml, 8ml and 10ml Ti/ZnO films respectively. These results suggest that there are improvements in the crystallite sizes as well as the dislocation densities of the deposited thin films as a result of Ti doping on the ZnO structure. These increments in the values of D and subsequent decrease in the values of δ by Ti doping are indicative of proper lattice positioning of the Ti atoms into the ZnO thin film crystal structure, improvement in crystallinity and reduction in the crystal defects in the deposited films.

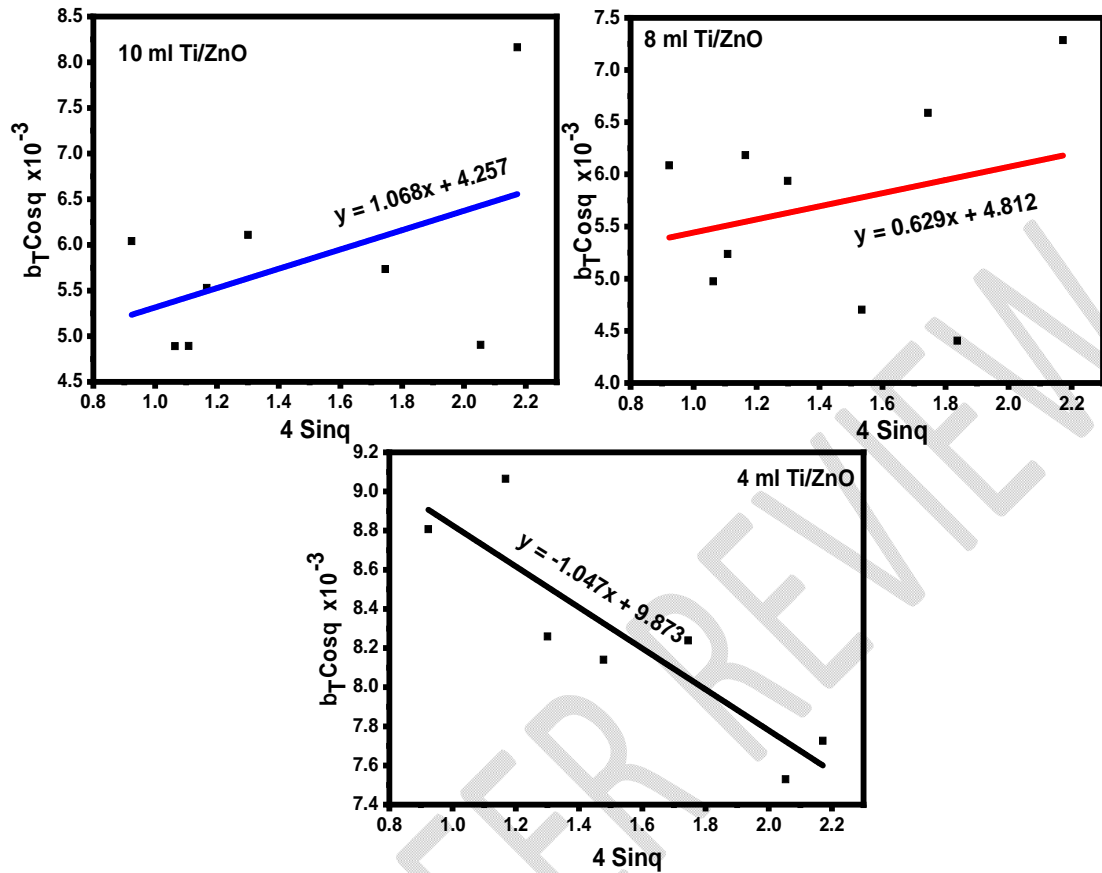


Figure 11: Williamson-Hall (W-H) analysis of the deposited Ti/ZnO thin films

Conclusion

The results of the optical and structural analysis of Ti doped ZnO thin films deposited in this work showed that the various properties of the films studied were influenced as a result of Ti doping. The deposited thin films Ti-ZnO exhibited very low absorbance and reflectance (%) in the VIS and NIR regions but the values for the films deposited at higher concentration of Ti increased in the VIS region. These low absorbance and reflectance were compensated with a high transmittance percentage values for the films in the VIS and NIR regions of electromagnetic spectrum. The refractive of the films is been altered differently both in the VIS and NIR range as result of Ti doping. The films formed with 10 ml Ti demonstrated higher value of refractive index (1.5-2.3) in the VIS but decreased to lowest value in the NIR. The deposited thin films Ti-ZnO has very low value of extinction coefficient but are greatly influenced by the concentration of Ti doping. The bandgap energies of the films are generally in the range 2.73 – 3.20 eV and were found to decrease as the volume concentration of Ti increased. The films deposited at higher concentrations of 6 ml, 8 ml and 10 ml Ti/ZnO has bandgap energies of 3.0 eV, 2.81 eV and 2.76 eV respectively. The results of the structural analysis showed that the films have crystalline structures. The crystallinity was found to increase as a result of Ti doping as there is increase in the number of sharp peaks as the concentration of Ti increased. The crystallite size increased with the Ti doping while there were records of minimal micro-strain and dislocation density at higher Ti concentration doping. These established results position the deposited thin films of Ti-ZnO for improved opto-electronic device applications.

References

- [1] Stoleriu, S., Lungu, C., Ghitulica, C. D., Surdu, A., Voicu, G., Cucuruz, A., ... & Ciocan, L. T. (2020). Influence of dopant nature on biological properties of ZnO thin-film coatings on Ti alloy substrate. *Nanomaterials*, 10(1), 129. Pg 1-15.
- [2] Akcan, D., Ozharar, S., Ozugurlu, E., & Arda, L. (2019). The effects of Co/Cu Co-doped ZnO thin films: An optical study. *Journal of Alloys and Compounds*, 797, 253-261.
- [3] Ramadan, R., Romera, D., Carrascón, R. D., Cantero, M., Aguilera-Correa, J. J., Garcia Ruiz, J. P., ... & Silván, M. M. (2019). Sol-gel-deposited Ti-doped ZnO: Toward cell fouling transparent conductive oxides. *ACS omega*, 4(7), 11354-11363.
- [4] Speaks D. K (2020). Effect of concentration, aging, and annealing on sol gel ZnO and Al-doped ZnO thin films. *International Journal of Mechanical and Materials Engineering*, 15:2, page 1-14. <https://doi.org/10.1186/s40712-019-0113-6>
- [5] Lu, J. J., Lu, Y. M., Tasi, S. I., Hsiung, T. L., Wang, H. P., & Jang, L. Y. (2007). Conductivity enhancement and semiconductor-metal transition in Ti-doped ZnO films. *Optical materials*, 29(11), 1548-1552.
- [6] Alias, M. F. A., Rashid, K. M., & Adem, K. A. (2014). Optical properties for Ti doped thin ZnO films prepared by PLD. *International Journal of Innovative Research in Science, Engineering and Technology*, 3(8), 15538-15544.
- [7] Benramache, S., Belahssen, O., & Temam, H. B. (2014). Effect of band gap energy on the electrical conductivity in doped ZnO thin film. *Journal of Semiconductors*, 35(7), 073001.
- [8] Mathew, J. P., Varghese, G., & Mathew, J. (2015, February). Effect of annealing on the optical properties of transition metal doped ZnO thin films. In *IOP Conference Series: Materials Science and Engineering* (Vol. 73, No. 1, pg 1-5).
- [9] Hafdallah, A., Ynineb, F., Aida, M. S., & Attaf, N. (2011). In doped ZnO thin films. *Journal of Alloys and Compounds*, 509(26), 7267-7270.
- [10] S. T. Tan, S. T, Chen, B. J, Sun, X. W and Fan, W. J (2005). Blueshift of optical band gap in ZnO thin films grown by metal-organic chemical-vapor deposition. *Journal of applied physics* 98, 1-5.
- [11] Bahşi, Z. B., & Oral, A. Y. (2007). Effects of Mn and Cu doping on the microstructures and optical properties of sol-gel derived ZnO thin films. *Optical Materials*, 29(6), 672-678.
- [12] Shao, Q., Wang, C., Zapien, J. A., Leung, C. W., & Ruotolo, A. (2015). Ferromagnetism in Ti-doped ZnO thin films. *Journal of Applied Physics*, 117(17), 1-5.
- [13] Chang, H. P., Wang, F. H., Chao, J. C., Huang, C. C., & Liu, H. W. (2011). Effects of thickness and annealing on the properties of Ti-doped ZnO films by radio frequency magnetron sputtering. *Current Applied Physics*, 11(1), S185-S190.
- [14] Bidier, S. A., Hashim, M. R., & Bououdina, M. (2017). Structural and optical characteristics of Ti-doped ZnO nanorods deposited by simple chemical bath deposition. *Journal of Materials Science: Materials in Electronics*, 28, 11178-11185.
- [15] Wang, F. H., Chang, H. P., & Chao, J. C. (2011). Improved properties of Ti-doped ZnO thin films by hydrogen plasma treatment. *Thin Solid Films*, 519(15), 5178-5182
- [16] Vorobyeva, N. A., Romyantseva, M. N., Vasiliev, R. B., Kozlovskiy, V. F., Soshnikova, Y. M., Filatova, D. G., ... & Gaskov, A. M. (2015). Doping effects on electrical and optical properties of spin-coated ZnO thin films. *Vacuum*, 114, 198-204.
- [17] Tseng, Y. C., Lin, Y. J., Chang, H. C., Chen, Y. H., Liu, C. J., & Zou, Y. Y. (2012). Effects of Ti content on the optical and structural properties of the Ti-doped ZnO nanoparticles. *Journal of Luminescence*, 132(2), 491-494.

- [18] Naeem, M., Qaseem, S., Gul, I. H., & Maqsood, A. (2010). Study of active surface defects in Ti doped ZnO nanoparticles. *Journal of applied physics*, 107(12).
- [19] Tseng, Y. C., Lin, Y. J., Chang, H. C., Chen, Y. H., Liu, C. J., & Zou, Y. Y. (2012). Effects of Ti content on the optical and structural properties of the Ti-doped ZnO nanoparticles. *Journal of Luminescence*, 132(2), 491-494.
- [20] Yong, Z., Liu, T., Uruga, T., Tanida, H., Qi, D., Rusydi, A., & Wee, A. T. (2010). Ti-doped ZnO thin films prepared at different ambient conditions: electronic structures and magnetic properties. *Materials*, 3(6), 3642-3653.
- [21] Lin, J. C., Huang, M. C., Wang, T., Wu, J. N., Tseng, Y. T., & Peng, K. C. (2015). Structure and characterization of the sputtered ZnO, Al-doped ZnO, Ti-doped ZnO and Ti, Al-co-doped ZnO thin films. *Materials Express*, 5(2), 153-158.
- [22] Lee, H. W., Choi, B. G., Shim, K. B., & Oh, Y. J. (2005). Preparation of Ti-doped ZnO transparent conductive thin films by PLD method. *Journal of Ceramic Processing & Research*, 6(1), 52-56.
- [23] Lee, D. J., Kim, K. J., Kim, S. H., Kwon, J. Y., Xu, J., & Kim, K. B. (2013). Atomic layer deposition of Ti-doped ZnO films with enhanced electron mobility. *Journal of Materials Chemistry C*, 1(31), 4761-4769.
- [24] Ye, Zhi-Yuan, Hong-Liang Lu, Yang Geng, Yu-Zhu Gu, Zhang-Yi Xie, Yuan Zhang, Qing-Qing Sun, Shi-Jin Ding, and David Wei Zhang(2013). Structural, electrical, and optical properties of Ti-doped ZnO films fabricated by atomic layer deposition." *Nanoscale research letters* 8, 1-6.
- [25] Nwori, A.N, Ezenwaka, L. N, Ottih, I. E, Okereke, N. A and Okoli, N. L (2022). Study of the Optical, Structural and Morphological Properties of Electrodeposited Copper Manganese Sulfide (CuMnS) Thin Films for Possible Device Applications, Trends in Sciences, Vol.19, No. 17, pp.5747-5747.
- [26] AfşinKariper, I, Özden, S, and Tezel, F. M. (2018). Optical properties of selenium sulfide thin film produced via chemical dropping method, Optical and Quantum Electronics, Vol. 50, pp. 1-7.
- [27] M. Rabiei, A. Palevicius, A. Monshi, S. Nasiri, A. Vilkauskas, G. Janusas, (2020). "Comparing methods for calculating nano crystal size of natural hydroxyapatite using X-ray diffraction," *Nanomaterials*, Vol.10, Issue 9, pp.1-21, 2020.
- [28] Ezenwaka, L.N, Nwori, A.N, Ottih, I. E, Okereke, N.A and Okoli, N. L (2022). Investigation of the Optical, Structural and Compositional Properties of Electrodeposited Lead Manganese Sulfide (PbMnS) Thin Films for Possible Device Applications," *Nanoarchitectonics*, pp.18-32.
- [29] Kalu U. A., Okpala U.V., Okereke N.a and Nwori A.N. (2023). Structural and Optical Properties of Black Velvet Tamarind Doped Magnesium Sulfide Thin Films Grown by Sol-Gel Technique. *Journal of Physics and Chemistry of Materials* Vol.10, Issue.4, pp.01-09.
- [30] Ikhioya, I.L, Ehika, S and Omehe, N. N (2018). Electrochemical deposition of lead sulphide (PbS) thin films deposited on zinc plate substrate, *Journal of Materials Science Research and Reviews*, Vol.1, No.3, pp.1-11.
- [31] Osanyinlusi, O. (2020). Preparation and Characterization of ZnS Thin Films Grown by Spin Coating Technique, *Tanzania J. Sci.* vol 46, no 2, pp 534-547.
- [32] Parajuli, D, Sandip Dangi, Bhumi Raj Sharma, Nunu Lal Shah and Devendra K. C. (2023). Sol-gel synthesis, characterization of ZnO thin films on different substrates, and bandgap calculation by the Tauc plot method. *BIBECHANA* Vol. 20, No. 2, 113–125.
- [33] Ohwofosirai, A, Femi D.M, Nwokike A.N, Toluchi, O.J, Osuji R. U and Ezekoye, B.A. (1014) "A Study of the Optical Conductivity, Extinction Coefficient and Dielectric Function of CdO by Successive Ionic Layer Adsorption and Reaction (SILAR) Techniques," *American Chemical Science Journal*, Vol. 4, No., 6, pp. 736-744.
- [34] Rajathi, S, Kirubavathi, K and Selvaraju K. (2017). Preparation of nanocrystalline Cd-doped PbS thin films and their structural and optical properties, *Journal of Taibah University for Science*, Vol. 11, No. 6, pp. 1296-1305.
- [35] Nwori, A.N., Ezenwaka L.N. Otti, E. I. Okereke, N.A. Okoli, N.L. (2021) Optical, Electrical, Structural and morphological Properties of Electrodeposited CdMnS Thin Film Semiconductors for Possible Device Applications. *Journal of Physics and Chemistry of Materials* Vol.8, Issue.2, pp.01-11.

- [36] Rajathi, S Kirubavathi K. and Selvaraju K (2017). Preparation of nanocrystalline Cd-doped PbS thin films and their structural and optical properties, Journal of Taibah University for Science, 11:6, 1296-1305, DOI: 10.1016/j.jtusci.2017.05.001.
- [37] Chauhan, R., Srivastava, A. K., Mishra, M., & Srivastava, K. K. (2010). Effect of UV exposure on some optical properties of As-Se based chalcogenide glasses. *Integrated Ferroelectrics*, 119(1), 22-32.
- [38] Chanthong, T, Intaratat, W and Wichean, T.N (2023). Effect of Thickness on Electrical and Optical Properties of ZnO: Al Films, Trends in Sciences, Vol.20, No. 3, pp.6372-6372
- [39] Nwori, A.N, Ezenwaka, L. N, Ottih, I. E, Okereke, N. A, Umeokwona, N. S, Okoli, N. L and Obimma, I.O (20210). Effect of Deposition Voltage Variation on the Optical Properties of PbMnS Thin Films Deposited by Electrodeposition Method," Journal of Physics and Chemistry of Materials, Vol.8, No. 3, pp.12-22.
- [40] M Rajasekaran, A Arunachalam and P Kumaresan (2020). Structural, morphological and optical characterization of Ti-doped ZnO nanorod thin film synthesized by spray pyrolysis technique. *Materials Research Express*, vol 7, page 1-17.
- [41] Gareso, P.L, Heryanto, H, Juarlin, E. Taba, P. (2023). Effect of Annealing on the Structural and Optical Properties of ZnO/ITO and AZO/ITO Thin Films Prepared by Sol-Gel Spin Coating," Trends in Sciences, Vol.20, Issue 3, pp.6521-6521.